

# A chiral bag model approach to delta electroproduction

D. H. Lu, A. W. Thomas, and A. G. Williams

*Department of Physics and Mathematical Physics, University of Adelaide, Australia 5005*

*and*

*Institute for Theoretical Physics, University of Adelaide, Australia 5005*

## Abstract

Helicity amplitudes for the  $\gamma^*N \rightarrow \Delta$  transition are calculated using the cloudy bag model. A correction for center-of-mass motion is carried out using a modified Peierls-Thouless projection method. This reduces the magnitude of the transition amplitudes at small momentum transfer and enhances them at modest momentum transfers. Our calculation shows that the pion cloud contributes substantially to the transition helicity amplitudes, with the final result giving reasonable agreement with the corresponding experimental values.

## I. INTRODUCTION

The nucleon-delta electromagnetic transition amplitude is an outstanding example of the success of the quark model [1]. There have been many theoretical and experimental explorations of this transition process. In a naive quark model the  $\gamma^*N \rightarrow \Delta$  transition occurs only by an M1 transition, while the E2 process is fully suppressed [2]. In more sophisticated models, quarks can interact through, for example, one-gluon exchange in addition to the confinement potential between them. Then it is possible for configuration mixing, involving the excitation of one quark to a  $d$ -state, to generate a small, but nonvanishing, E2

amplitude [3]. To extract the  $\gamma^*N \rightarrow \Delta$  amplitude from experimental data is not an easy task. There are some uncertainties on the subtraction of background, and the results are somewhat model dependent [4]. With the advent of new generation of accelerators, much more accurate measurements will be made. The prospect of the high quality data should test various hadron models well and help to build more realistic ones.

The cloudy bag model (CBM) [5] improves the MIT bag model [6] by introducing an elementary, perturbative pion field which couples to quarks in the bag in such a way that chiral symmetry is restored. The pion field significantly improves the predictions of the static properties of baryons. It also provides a convenient connection to the traditional language in nuclear physics. Kalbermann and Eisenberg (KE) [7] first used the cloudy bag model to calculate the photoproduction of delta and Roper resonances at the threshold. They showed that the pionic corrections can substantially improve the predictions of the helicity amplitudes. Subsequently Bermuth et al. [8] updated the KE calculation with some algebraic corrections and the appropriate normalization of baryon states. By comparing pseudoscalar (PS) and pseudovector (PV) coupling versions of the CBM, they found that the two are almost identical for the M1 transition, except for the seagull term, which actually spoils the good fit to the experimental data. The recoil effects were neglected in both calculations, which were limited to photoproduction at the peak of the delta resonance.

In the standard treatment of the cloudy bag model, the cavity approximation for quark fields is adopted, and the pion field is then added in a perturbative way. The wave function of a bare baryon is just a direct product of individual quark wave functions, similar to the nuclear shell-model wave function (independent particle motion). This type of wave function is not a momentum eigenstate although the Hamiltonian commutes with the total momentum operator. The matrix elements evaluated between such static states contain spurious center of mass motion which ought to be removed. Early studies indicated that the correction for spurious center of mass motion is significant [9]. It is expected to be most important in calculations where relatively large momentum transfers are involved. There are several intuitively motivated prescriptions [9] for the correction of center of mass

motion, however, none of them are fully satisfactory. In this work, we have chosen to use the Peierls-Thouless (PT) [10] method to eliminate the center of mass motion, since it is the most convenient for our purposes. It is basically a nonrelativistic approach and requires two consecutive projections of the product wave functions to form a Galilean invariant state for a composite baryon. The energy expectation value evaluated using the PT projected wave function has the correct nonrelativistic form, whereas this is not the case for Peierls-Yoccoz projection.

In this paper, we calculate the nucleon-delta electromagnetic transition amplitudes with respect to the virtual photon. The spurious center of mass motion is corrected by using the PT projection method. As a first step, we assume exact  $SU(6)$  symmetry for the quark structure of the baryons, so that all quarks in the ground state of  $N$  and  $\Delta$  are in the  $s$  state. The notation of references [11,12] is followed. We briefly review the method to construct the PT wave function in Sec. II. The calculation of helicity amplitudes for virtual photoproduction of the delta is performed in Sec. III, and in Sec. IV we present the numerical results. Finally in Sec. V we summarize our results.

## II. GALILEAN INVARIANT BARYON STATES

We start with the chirally invariant Lagrangian density of the cloudy bag model [5]

$$\begin{aligned} \mathcal{L} = & (i\bar{q}\gamma^\mu\partial_\mu q - B)\theta_V - \frac{1}{2}\bar{q}q\Delta_S \\ & + \frac{1}{2}(\partial_\mu\boldsymbol{\pi})^2 - \frac{1}{2}m_\pi^2\boldsymbol{\pi}^2 - \frac{i}{2f}\bar{q}\gamma_5\boldsymbol{\tau}\cdot\boldsymbol{\pi}q\Delta_S, \end{aligned} \quad (1)$$

where  $\theta_V$  is a step function which is one inside the bag volume  $V$  and vanishes outside, and  $\Delta_S$  is a surface delta function. In a perturbative treatment of the pion field, the quark wave function is not affected by the pion field and is given by the MIT bag solution [6]

$$q(\mathbf{r}) = \begin{pmatrix} g(r) \\ i\boldsymbol{\sigma}\cdot\hat{\mathbf{r}}f(r) \end{pmatrix} \theta(R-r), \quad (2)$$

where  $R$  is the spherical bag radius. For the ground state of a massless quark  $g(r) = N_s j_0(\omega_s r/R)$ ,  $f(r) = N_s j_1(\omega_s r/R)$ , where  $\omega_s = 2.0428$  and  $N_s^2 = \omega_s/8\pi R^3 j_0^2(\omega_s)(\omega_s - 1)$ .

The bare baryon is taken to be composed of three quarks with the spin-flavor wave function given by  $SU(6)$  symmetry. The space component is naively the direct product of three quark wave functions in coordinate space

$$\Psi(\mathbf{x}_1, \mathbf{x}_2, \mathbf{x}_3; \mathbf{x}) = q(\mathbf{x}_1 - \mathbf{x})q(\mathbf{x}_2 - \mathbf{x})q(\mathbf{x}_3 - \mathbf{x}). \quad (3)$$

Here  $\mathbf{x}$  indicates the location of the bag center, while  $\mathbf{x}_1$ ,  $\mathbf{x}_2$ , and  $\mathbf{x}_3$  specify the positions of the three quarks. Clearly this wavefunction does not have definite momentum and is not a momentum eigenstate. A momentum eigenstate of the baryon can be constructed by making a linear superposition of the localized states, namely,

$$\Psi_{\text{PY}}(\mathbf{x}_1, \mathbf{x}_2, \mathbf{x}_3; \mathbf{p}) = N'(p) \int d^3\mathbf{x} e^{i\mathbf{p}\cdot\mathbf{x}} \Psi(\mathbf{x}_1, \mathbf{x}_2, \mathbf{x}_3; \mathbf{x}), \quad (4)$$

where the subscript PY stands for Peierls-Yoccoz projection [13], and  $N'(p)$  is a momentum dependent normalization constant. It can be shown that  $\Psi_{\text{PY}}(\mathbf{p}) = e^{i\mathbf{p}\cdot\mathbf{x}_{\text{cm}}} \Psi_{\text{in}}(\mathbf{p})$ , where  $\mathbf{x}_{\text{cm}} = (\mathbf{x}_1 + \mathbf{x}_2 + \mathbf{x}_3)/3$  is the center of mass of the baryon and  $\Psi_{\text{in}}(\mathbf{p})$  is the appropriately defined intrinsic part of the wave function. Since  $\Psi_{\text{in}}(\mathbf{p})$  still depends on the c.m. momentum, it violates translational invariance. To overcome this problem, Peierls and Thouless (PT) [10] proposed to make another superposition of these momentum eigenstates, i.e.,

$$\Psi_{\text{PT}}(\mathbf{x}_1, \mathbf{x}_2, \mathbf{x}_3; \mathbf{p}) = N(p) \int d^3p' w(\mathbf{p}') e^{i(\mathbf{p}-\mathbf{p}')\cdot\mathbf{x}_{\text{cm}}} \Psi_{\text{PY}}(\mathbf{x}_1, \mathbf{x}_2, \mathbf{x}_3; \mathbf{p}'). \quad (5)$$

The weight function,  $w(p')$ , should in fact be chosen to minimize the total energy, but this would be quite complicated to implement here. Instead, we choose  $w(\mathbf{p}') = 1$  for simplicity and convenience. Then integrations over  $\mathbf{x}$  and  $\mathbf{p}'$  can be carried out easily. This leads to a much simplified PT wave function,

$$\Psi_{\text{PT}}(\mathbf{x}_1, \mathbf{x}_2, \mathbf{x}_3; \mathbf{p}) = N_{\text{PT}} e^{i\mathbf{p}\cdot\mathbf{x}_{\text{cm}}} q(\mathbf{x}_1 - \mathbf{x}_{\text{cm}}) q(\mathbf{x}_2 - \mathbf{x}_{\text{cm}}) q(\mathbf{x}_3 - \mathbf{x}_{\text{cm}}), \quad (6)$$

where the normalization factor,  $N_{\text{PT}}$ , is given by the condition

$$\int d^3x_1 d^3x_2 d^3x_3 \Psi_{\text{PT}}^\dagger(\mathbf{x}_1, \mathbf{x}_2, \mathbf{x}_3; \mathbf{p}') \Psi_{\text{PT}}(\mathbf{x}_1, \mathbf{x}_2, \mathbf{x}_3; \mathbf{p}) = (2\pi)^3 \delta^{(3)}(\mathbf{p}' - \mathbf{p}). \quad (7)$$

This leads to

$$N_{\text{PT}} = \left[ 3 \int d^3r_1 d^3r_2 \rho(\mathbf{r}_1) \rho(\mathbf{r}_2) \rho(-\mathbf{r}_1 - \mathbf{r}_2) \right]^{-1/2}, \quad (8)$$

where  $\rho(\mathbf{r})$ , the quark density at the position  $\mathbf{r}$ , is defined as

$$\rho(\mathbf{r}) \equiv q^\dagger(\mathbf{r})q(\mathbf{r}) = [g^2(r) + f^2(r)] \theta(R - r). \quad (9)$$

Notice that, for this simple version of the PT projection,  $N_{\text{PT}}$  is a momentum independent constant and the wavefunction in Eq. (6) is manifestly Galilean invariant.

### III. THE HELICITY AMPLITUDES IN THE CLOUDY BAG MODEL

From the CBM Lagrangian given in Eq. (1), the conserved local electromagnetic current can be derived using the principle of minimal coupling  $\partial_\mu \rightarrow \partial_\mu + iqA_\mu$ , where  $q$  is the charge carried by the field upon which the derivative operator acts. The total electromagnetic current is then

$$J^\mu(x) = j_q^\mu(x) + j_\pi^\mu(x), \quad (10)$$

$$j_q^\mu(x) = \sum_a Q_a e \bar{q}_a(x) \gamma^\mu q_a(x), \quad (11)$$

$$j_\pi^\mu(x) = -ie[\pi^\dagger(x) \partial^\mu \pi(x) - \pi(x) \partial^\mu \pi^\dagger(x)], \quad (12)$$

where  $q_a(x)$  is the quark field operator for flavor  $a$ ,  $Q_a$  is its charge in units of  $e$ , and  $e \equiv |e|$  is the magnitude of the electron charge. The charged pion field operator is defined as

$$\pi(x) = \frac{1}{\sqrt{2}}[\pi_1(x) + i\pi_2(x)], \quad (13)$$

where  $\pi(x)$  either destroys a negatively charged pion or creates a positively charged one.

It is customary to define the helicity amplitudes for the electroproduction of the delta as [14]

$$A_{3/2} = \frac{1}{\sqrt{2\omega_\gamma}} \langle \Delta; s_\Delta = 3/2 | \vec{J}(0) \cdot \vec{\epsilon} | N; s_N = 1/2 \rangle, \quad (14)$$

$$A_{1/2} = \frac{1}{\sqrt{2\omega_\gamma}} \langle \Delta; s_\Delta = 1/2 | \vec{J}(0) \cdot \vec{\epsilon} | N; s_N = -1/2 \rangle, \quad (15)$$

where the  $\Delta$  is at rest and the photon is travelling along the z-axis with right-handed polarization,  $\vec{\epsilon} = -\frac{1}{\sqrt{2}}(1, i, 0)$ . The spin projections of  $\Delta$  and  $N$  along the z-axis are denoted as  $s_\Delta$  and  $s_N$  respectively. For a virtual photon, the three-momentum in the  $\Delta$  rest frame is given by

$$|\vec{q}|^2 = Q^2 + \frac{(M_\Delta^2 - M_N^2 - Q^2)^2}{4M_\Delta^2}, \quad (16)$$

with  $Q = \sqrt{-q^2}$  the magnitude of the four momentum transfer. The photon energy is related to this by  $q_0^2 = |\vec{q}|^2 - Q^2$ , where for a real photon we have  $Q^2 = 0$ , so that  $\omega_\gamma = |q_0| = (M_\Delta^2 - M_N^2)/2M_\Delta$ .

The experimentally extracted, resonant, helicity amplitudes are to be associated with the fully dressed initial and final baryons. In the cloudy bag model, due to the  $\pi BB'$  coupling, a physical baryon state is described as a mixture of a bare bag and its surrounding pion cloud,

$$|A\rangle = \sqrt{Z_2^A} [1 + (E_A - H_0 - \Lambda H_I \Lambda)^{-1} H_I] |A_0\rangle, \quad (17)$$

where  $Z_2^A$  is the bare baryon probability in the physical baryon states,  $\Lambda$  is a projection operator which projects out all the components of  $|A\rangle$  with at least one pion, and  $H_I$  is the interaction Hamiltonian which describes the process of emission and absorption of pions. The matrix elements of  $H_I$  between the bare baryon states and their properties are then given by [11,12]

$$v_{0j}^{AB}(\vec{k}) \equiv \langle A_0 | H_I | \pi_j(\vec{k}) B_0 \rangle = \frac{if_0^{AB}}{m_\pi} \frac{u(kR)}{[2\omega_k(2\pi)^3]^{1/2}} \sum_{m,n} C_{S_B 1 S_A}^{s_B m s_A}(\hat{s}_m^* \cdot \vec{k}) C_{T_B 1 T_A}^{t_B n t_A}(\hat{t}_n^* \cdot \vec{e}_j), \quad (18)$$

$$w_{0j}^{AB}(\vec{k}) \equiv \langle A_0 \pi_j(\vec{k}) | H_I | B_0 \rangle = [v_{0j}^{BA}(\vec{k})]^* = -v_{0j}^{AB}(\vec{k}) = v_{0j}^{AB}(-\vec{k}), \quad (19)$$

where the pion has momentum  $\vec{k}$  and isospin projection  $j$ ,  $f_0^{AB}$  is the reduced matrix element for the  $\pi B_0 \rightarrow A_0$  transition vertex,  $u(kR) = 3j_1(kR)/kR$ ,  $\omega_k = \sqrt{k^2 + m_\pi^2}$ , and  $\hat{s}_m$  and  $\hat{t}_n$  are spherical unit vectors for spin and isospin, respectively.

Under the approximation that there is at most one pion in the air, there are three different processes contributing to the  $\gamma^*N \rightarrow \Delta$  vertex, as shown in Fig. 1. Substituting the quark current operator, Eq. (11), and the physical baryon states, Eq. (17), into Eqs. (14) and (15), we have

$$\begin{aligned} \langle \Delta, s_\Delta | \vec{j}_q \cdot \vec{\epsilon} | N, s_N \rangle &= \sqrt{Z_2^N Z_2^\Delta} \left[ \langle \Delta_0, s_\Delta | \vec{j}_q \cdot \vec{\epsilon} | N_0, s_N \rangle \right. \\ &\left. + \langle \Delta_0, s_\Delta | H_I (E - H_0 - \Lambda H_I \Lambda)^{-1} \vec{j}_q \cdot \vec{\epsilon} (E - H_0 - \Lambda H_I \Lambda)^{-1} H_I | N_0, s_N \rangle \right] \end{aligned} \quad (20)$$

where  $E$  is the total energy of this transition process. The first term, as illustrated in Fig. 1(a), is the quark core contribution and the second term, corresponding to Fig. 1(b), is the contribution from the  $\gamma qq$  interaction with one  $\pi$  in the air. By inserting two complete sets of states before and after the operator  $\vec{j}_q$  in the second term and using the PT wavefunctions given in Eq. (6), we obtain

$$\begin{aligned} A_{3/2}^{(a)}(Q^2) &= \sqrt{3} A_{1/2}^{(a)}(Q^2) = A_{\text{bare}}(Q^2) \sqrt{Z_2^N Z_2^\Delta}, \quad (21) \\ A_{3/2}^{(b)}(Q^2) &= \sqrt{3} A_{1/2}^{(b)}(Q^2) = A_{\text{bare}}(Q^2) \frac{(f^{NN})^2}{27\pi^2 m_\pi^2} \int \frac{dk k^4 u^2(kR)}{\omega_k} \left[ \frac{5/4}{\omega_k(\omega_k + \delta - \omega_\gamma)} \right. \\ &\quad \left. + \frac{1}{(\omega_k + \delta)(\omega_k + \delta - \omega_\gamma)} + \frac{2/25}{(\omega_k + \delta)(\omega_k - \omega_\gamma)} + \frac{1}{\omega_k(\omega_k - \omega_\gamma)} \right], \quad (22) \end{aligned}$$

where  $\delta = m_\Delta - m_N$ , and  $f^{NN}$  is the renormalized  $\pi NN$  coupling constant. The four terms in the right-hand side of Eq. (22) correspond to four possible intermediate states,  $(N\Delta)$ ,  $(\Delta\Delta)$ ,  $(\Delta N)$ , and  $(NN)$ , respectively. The recoil corrected bare  $\gamma N_0 \rightarrow \Delta_0$  transition amplitude is

$$A_{\text{bare}}(Q^2) = -\frac{e}{\pi\sqrt{6}\omega_\gamma} \frac{\int_0^R dr r^2 g(r) f(r) j_1(qr) K(r)}{\int_0^R dr r^2 \rho(r) K(r)}, \quad (23)$$

where  $K(r) = \int d^3x \rho(\vec{x}) \rho(-\vec{x} - \vec{r})$  is the recoil function to account for the correlation of the two spectator quarks. The renormalization constants,  $Z_2^A$ , are determined by the normalization condition for the physical baryon state, i.e.

$$Z_2^A = \left[ 1 - \frac{\partial}{\partial E} \Sigma^A(E) \right]_{E=m_A}^{-1}, \quad (24)$$

where  $\Sigma^A$ , the self energy of the baryon  $A$ , is given by

$$\Sigma^A(E) = \sum_B \left( \frac{f_0^{AB}}{m_\pi} \right)^2 \frac{1}{12\pi^2} \text{P} \int \frac{dk k^4 u^2(kR)}{\omega_k(E - m_B - \omega_k)}, \quad (25)$$

where P indicates that the principle part of the integral is to be taken. In this work, we have adopted the usual philosophy for the renormalization in the CBM. Throughout this work approximate relation,  $f^{AB} \simeq \left( \frac{f_0^{AB}}{f_0^{NN}} \right) f^{NN}$ , is always used. There are uncertain corrections on the bare coupling constant  $f_0^{NN}$ , such as the nonzero quark mass and correction of center of mass motion. Therefore, we use the renormalized coupling constant in our calculation,  $f^{NN} \simeq 3.03$ , which correspond to the usual  $\pi NN$  coupling constant,  $f_{\pi NN}^2 \simeq 0.081$ . As a result, the factor  $\sqrt{Z_2^N Z_2^A}$  is absorbed into the renormalized coupling constants in Fig. 1(b). This treatment is equivalent to the original CBM formalism up to order  $(f^{NN})^2$  and consistent with current conservation.

To evaluate the contribution caused by the photon-pion-pion coupling vertex [see Fig. 1(c)], we use the usual plane wave expansion for the quantized pion field

$$\pi_j(\vec{x}, t=0) = \int \frac{d^3k}{[(2\pi)^3 2\omega_k]^{1/2}} \left[ a_j(\vec{k}) e^{i\vec{k}\cdot\vec{x}} + a_j^\dagger(\vec{k}) e^{-i\vec{k}\cdot\vec{x}} \right], \quad (26)$$

where  $a_j(\vec{k})$  ( $a_j^\dagger(\vec{k})$ ) annihilates (creates) a pion with momentum  $\vec{k}$  and isospin  $j$ . The pion current operator becomes

$$\vec{j}_\pi(\vec{x}) = -ie \sum_{jj'} \epsilon_{jj'3} \int \frac{d^3k d^3k'}{(2\pi)^3 2(\omega_k \omega_{k'})^{1/2}} \vec{k} e^{i(\vec{k}-\vec{k}')\cdot\vec{x}} \left[ a_{j'}(-\vec{k}') + a_{j'}^\dagger(\vec{k}') \right] \cdot \left[ a_j(\vec{k}) + a_j^\dagger(-\vec{k}) \right]. \quad (27)$$

The transition amplitude at position  $\vec{x}$  is just the matrix element of  $\vec{j}_\pi(\vec{x})$  evaluated between the physical baryon states. Using the identities

$$a_j(\vec{k})|A\rangle = (E_A - \omega_k - H)^{-1} V_{0j}^\dagger(\vec{k})|A\rangle, \quad (28)$$

$$\begin{aligned} a_{j'}(\vec{k}') a_j(\vec{k})|A\rangle &= (E_A - \omega_k - \omega_{k'} - H)^{-1} V_{0j}^\dagger(\vec{k}) (E_A - \omega_{k'} - H)^{-1} V_{0j'}^\dagger(\vec{k}') \\ &+ (E_A - \omega_k - \omega_{k'} - H)^{-1} V_{0j'}^\dagger(\vec{k}') (E_A - \omega_k - H)^{-1} V_{0j}^\dagger(\vec{k})|A\rangle, \end{aligned} \quad (29)$$

we have



$$\begin{aligned}
\langle \Delta, s_\Delta | \vec{j}_\pi(\vec{x}) | N, s_N \rangle &= -ie \sum_{jj'} \epsilon_{jj'3} \int d^3k d^3k' e^{i(\vec{k}-\vec{k}')\cdot\vec{x}} \frac{\vec{k}}{(2\pi)^3 2(\omega_k \omega_{k'})^{1/2}} \\
&\times \sum_B \left[ \eta_{jj'}^B(\vec{k}', \vec{k}) G^B(\vec{k}', \vec{k}) + \eta_{jj'}^B(\vec{k}, \vec{k}') G^B(\vec{k}, \vec{k}') \right]. \tag{30}
\end{aligned}$$

Here  $B$  denotes the intermediate baryon states (restricted to  $N$  and  $\Delta$  here), and

$$\begin{aligned}
\eta_{jj'}^B(\vec{k}', \vec{k}) &\equiv \frac{f^{\Delta B} f^{NB}}{m_\pi^2} \frac{u(kR)u(k'R)}{16\pi^3(\omega_k \omega_{k'})^{1/2}} \\
&\times \sum_{s_B} C_{S_B 1 S_\Delta}^{s_B m' s_\Delta} C_{S_B 1 S_N}^{s_B m s_N} (\hat{s}_{m'} \cdot \mathbf{k}') (\hat{s}_m \cdot \mathbf{k}) \sum_{t_B} C_{T_B 1 T_\Delta}^{t_B n' t_\Delta} C_{T_B 1 T_N}^{t_B n t_N} (\hat{t}_{n'} \cdot \mathbf{e}_j) (\hat{t}_n \cdot \mathbf{e}_j), \tag{31}
\end{aligned}$$

$$G^N(\vec{k}', \vec{k}) \equiv \frac{1}{(\omega_k + \omega_{k'} + \delta)\omega_k} + \frac{1}{(\omega_{k'} - \omega_\gamma)\omega_k} + \frac{1}{(\omega_{k'} - \omega_\gamma)(\omega_k + \omega_{k'} - \omega_\gamma)}, \tag{32}$$

$$\begin{aligned}
G^\Delta(\vec{k}', \vec{k}) &\equiv \frac{1}{(\omega_k + \omega_{k'} + \delta)(\omega_k + \delta)} + \frac{1}{(\omega_{k'} + \delta - \omega_\gamma)(\omega_k + \delta)} \\
&+ \frac{1}{(\omega_{k'} + \delta - \omega_\gamma)(\omega_k + \omega_{k'} - \omega_\gamma)}. \tag{33}
\end{aligned}$$

$G^\Delta(\vec{k}, \vec{k}')$  and  $G^\Delta(\vec{k}', \vec{k})$  are obtained by the interchange of  $\vec{k}$  and  $\vec{k}'$  in the corresponding equation. The three terms appearing in Eqs. (32) and (33) correspond to the three different time orders in the time-ordered perturbation theory, as illustrated in Fig. 1(c). Using the translational invariance of the electromagnetic current operator,  $j^\mu(x) = e^{i\hat{p}\cdot x} j^\mu(0) e^{-i\hat{p}\cdot x}$ , then the  $\gamma^* N \rightarrow \Delta$  helicity amplitudes due to the  $\gamma\pi\pi$  interaction are simply given by

$$A(Q^2) = \int d^3x e^{i\vec{q}\cdot\vec{x}} \langle \Delta, s_\Delta | \vec{j}_\pi(\vec{x}) \cdot \vec{\epsilon} | N, s_N \rangle. \tag{34}$$

After performing some spin and isospin algebra, we obtain

$$\begin{aligned}
A_{3/2}^{(c)}(Q^2) &= -\frac{(f^{NN})^2 |\vec{q}|}{240\sqrt{6}\omega_\gamma \pi^3 m_\pi^2} \int \frac{d^3k k^4 \sin^2\theta u(kR)u(k'R)}{\omega_k \omega_{k'}} \\
&\times \left[ G^N(\vec{k}, \vec{k}') + 3G^\Delta(\vec{k}', \vec{k}) + 2G^\Delta(\vec{k}, \vec{k}') \right], \tag{35}
\end{aligned}$$

$$\begin{aligned}
A_{1/2}^{(c)}(Q^2) &= -\frac{(f^{NN})^2 |\vec{q}|}{720\sqrt{2}\omega_\gamma \pi^3 m_\pi^2} \int \frac{d^3k k^4 \sin^2\theta u(kR)u(k'R)}{\omega_k \omega_{k'}} \\
&\times \left[ 2G^N(\vec{k}', \vec{k}) - G^N(\vec{k}, \vec{k}') + G^\Delta(\vec{k}', \vec{k}) + 4G^\Delta(\vec{k}, \vec{k}') \right], \tag{36}
\end{aligned}$$

where  $\vec{k}' = \vec{k} + \vec{q}$ ,  $\omega_{k'} = \sqrt{k'^2 + m_\pi^2}$ , and  $\theta$  denotes the angle between  $\vec{k}$  and  $\vec{q}$ . It is worthwhile to mention that the form of our results for Fig. 1(c) are expressed in a quite different form than those of KE [7] and Bermuth et al. [8] where the integral variables are  $k$  and  $k'$  in

their formulation. We believe that our expressions are more straightforward and manifestly respect the three momentum conservation at the  $\gamma\pi\pi$  vertex. Our numerical results for this contribution also appear to differ from those of Refs. [7,8].

#### IV. NUMERICAL RESULTS

Figure 2 shows the recoil function  $K(r)$  due to the two quark spectators. It cuts down the contributions from the quark wave functions near the bag boundary by up to 50 %. The overall effect of this recoil correction on the bare bag contribution to the typical  $\gamma^*N \rightarrow \Delta$  helicity amplitude,  $A_{3/2}$ , is shown in Fig. 3. In the real photon limit ( $Q^2 \rightarrow 0$ ), the magnitude of the  $\gamma^*N \rightarrow \Delta$  transition amplitude increases with the bag radii in a fashion similar to that of the magnetic moment of bare baryons. The correction of the center of mass motion usually reduces the bare transition amplitudes by 5 to 10 % for  $Q^2 \lesssim 0.5 \text{ GeV}^2$  within a reasonable range of bag radii. However, this recoil correction would flip sign and increase the transition amplitude for larger momentum transfers.

The expressions of  $A^{(b)}$  and  $A^{(c)}$  (from Fig. 1(b) and 1(c) respectively) involve pion-loop integrals, which contain poles originating from the baryon mass difference in the propagators.

Using the relation  $\text{P} \int_0^\infty \frac{dk}{k^2 - k_0^2} = 0$ , it can be shown that

$$\lim_{\epsilon \rightarrow 0^+} \int_0^\infty \frac{dk f(k)}{k^2 - k_0^2 - i\epsilon} = \int_0^\infty dk \frac{f(k) - f(k_0)}{k^2 - k_0^2} + \frac{i\pi}{2k_0} f(k_0), \quad (37)$$

where  $k_0 > 0$ . To be consistent with the phenomenology of the cloudy bag model, we limit our calculation to the small momentum transfer region (approximately  $Q^2 \lesssim 1.6 \text{ GeV}^2$ ). For higher momentum transfers, relativistic effects are essential and the support of the  $\theta$  integral is considerably more complicated. Consequently, for our purposes, there is only one relevant pole,  $\omega_k = \omega_\gamma$ , for Fig. 1(b) and an extra pole,  $\omega_{k'} = \omega_\gamma$ , for Fig. 1(c).

Fig. 4 shows the individual contributions to the helicity amplitude,  $A_{3/2}$ , from the various diagrams for a typical bag radius,  $R = 0.8 \text{ fm}$ . It is clear that the contributions from the pion cloud are significant in the cloudy bag model. As  $Q^2 \rightarrow 0$ , the pionic effects account

for two thirds of the total amplitude, or roughly twice that of the quark core for the chosen bag radius. As  $Q^2$  increases beyond  $0.2 \text{ GeV}^2$ , the contribution from the  $\gamma\pi\pi$  interaction decreases rather rapidly, so that it has nearly vanished at  $Q^2 \sim 1.2 \text{ GeV}^2$ . For  $Q^2 \gtrsim 1 \text{ GeV}^2$ , the pionic effects contribute about 40 % of the total amplitude. Notice that, since the  $\Delta$  is a resonance, the helicity amplitudes are actually complex. In the CBM the imaginary part arises from thresholds in the pion loop integral, and amounts to  $15 \sim 20\%$  of the real part.

The real parts of total helicity amplitudes,  $A = A^{(a)} + A^{(b)} + A^{(c)}$ , are presented in Fig. 5. With the contributions of the pion cloud, the bag radius dependence is quite different from that for the bare transition amplitudes shown in Fig. 3. This can be explained by the fact that the pionic contribution is competing with that of quark core, since a small bag radius means a strong pion cloud. In the small  $Q^2$  region, the pion cloud compensates more than the loss in the bare amplitude when using a small bag radius. Generally, the smaller the bag radius, the larger the total transition amplitude. We list the helicity amplitudes corresponding to the real photon limit at the  $\Delta$  resonance in Table 1. With the small bag radius  $R = 0.7 \text{ fm}$ , we are able to reproduce the experimental helicity amplitude in this model.

Finally, in Fig. 6, we show the real part of the invariant  $\gamma^*N \rightarrow \Delta$  magnetic transition form factor,  $G_{\Delta}^M(Q^2)$ , in comparison with the experimental measurements [16]. The relation between the helicity amplitudes and the invariant transition form factors are given in Ref. [17]. With the bag radius  $R = 1 \text{ fm}$ , our calculation agrees reasonably well with the data for modest  $Q^2$ , but is less satisfactory at  $Q^2 \simeq 0 \text{ GeV}^2$  and in the region  $Q^2 \gtrsim 1 \text{ GeV}^2$ . At the real photon limit, we are able to get the PDG [15] value with  $R = 0.7 \text{ fm}$ , however, at nonzero  $Q^2$  the prediction with this bag radius would not be in agreement with the data. The center of mass correction reduces  $G_{\Delta}^M(0)$  by approximately 5 % and makes the M1 form factor somewhat harder, similar to what was found in the case of the nucleon magnetic form factor [18].

In the present work the quark cores of nucleon and delta were assumed to have SU(6) symmetry, i.e., there is no deformation assumed, so that the spatial parts of the wave

functions for the  $N$  and  $\Delta$  are purely  $s$  state. Hence, here the only possible source for an  $E2$  amplitude is from Fig. 1(c). Using Eqs. (21), (22), (35) and (36), we obtain  $E2/M1 = (A_{1/2} - A_{3/2}/\sqrt{3})/(A_{1/2} + \sqrt{3}A_{3/2}) \sim -0.3 \times 10^{-3}$ . Because of the severe cancellation in the numerator, this result is about two orders of magnitude smaller than the phenomenological approach [4,15] (The latest estimate by Particle Data Group is  $-0.015 \pm 0.004$ ).

## V. SUMMARY

In conclusion, we have calculated the  $\gamma^* N \rightarrow \Delta$  transition form factors in the cloudy bag model, including the center of mass correction via a simplified Peierls-Thouless projection method. The effect of this recoil correction is to slightly reduce the magnetic form factor at small momentum transfer and to make the form factor slightly harder. Generally, with the PT projection the transition moment is reduced by about  $5 \sim 8\%$ .

The pion cloud contribution proved to be crucial to account for the measured helicity amplitudes using a reasonable bag radius in this model. In similar calculations using constituent quark models (the nonrelativistic [3] and relativized quark models [17]), the helicity amplitudes are usually significantly underpredicted.

Because of the large range of momentum transfer measured, we have been unable to obtain a totally satisfactory description of all of the data using our essentially nonrelativistic formalism. Typically the form factors are too stiff. Unfortunately, there is as yet no covariant formalism for quark bag models or soliton bag models. Using a relatively simple prescription for Lorentz boosts [19], the invariant form factor  $G_{\Delta}^M(Q^2)$  has shown improved behaviour. Obviously a crucial next step will be to construct a quark model with improved Lorentz transformation properties, in addition to the inclusion of a perturbative pion cloud. It will also be important to explore the effect of  $SU(6)$  violating admixtures in the baryon wave functions [3].

This work was supported by the Australian Research Council.

## REFERENCES

- [1] F. E. Close, *An Introduction to Quarks and Partons* (Academic Press, London, 1979).
- [2] C. M. Becchi and G. Morpurgo, Phys. Lett. **17**, 352 (1965).
- [3] N. Isgur, G. Karl, and R. Koniuk, Phys. Rev. D**25**, 2394 (1982); R. Koniuk and N. Isgur, Phys. Rev. D**21**, 1868 (1980).
- [4] R. M. Davidson, N. C. Mukhopadhyay, and R. S. Wittman, Phys. Rev. D**43**, 71 (1991).
- [5] A. W. Thomas, Adv. in Nucl. Phys. **13**, 1 (1984).
- [6] A. Chodos, R. L. Jaffe, K. Johnson, C. B. Thorn and V. F. Weisskopf, Phys. Rev. D**9**, 3471 (1974); A. Chodos, R. L. Jaffe, K. Johnson and C. B. Thorn, Phys. Rev. D**10**, 2599 (1974); T. A. DeGrand, R. L. Jaffe, K. Johnson and J. Kiskis, Phys. Rev. D**12**, 2060 (1975).
- [7] G. Kalbermann and J. M. Eisenberg, Phys. Rev. D**28**, 71 (1983).
- [8] K. Bermuth, D. Dreschsel, L. Tiator, and J. B. Seaborn, Phys. Rev. D**37**, 89 (1986).
- [9] L. Wilets, *Non-Topological Solitons* (World Scientific, Singapore, 1989); M. C. Birse, Prog. in Part. and Nucl. Phys. **25**, 1 (1990).
- [10] R. E. Peierls and D. J. Thouless, Nucl. Phys. **38**, 154 (1962).
- [11] S. Theberge and A. W. Thomas, Nucl. Phys. A**393**, 252 (1983); S. Theberge, G. A. Miller, and A. W. Thomas, Can. J. Phys. **60**, 59 (1982).
- [12] S. Theberge, Ph. D. Thesis (1982).
- [13] R. E. Peierls and J. Yoccoz, Proc. Phys. Soc. **70**, 381 (1957).
- [14] M. Bourdeau and N. C. Mukhopadhyay, Phys. Rev. Lett. **58**, 976 (1987).
- [15] Particle Data Group, Phys. Rev. D**54**, 601 (1996).

- [16] S. Stein et al., Phys. Rev. **D12**, 1884 (1976); W. Bartel et al., Phys. Lett. **B28**, 148 (1968).
- [17] M. Warns, H. Schroder, W. Pfeil, and H. Rollnik, Z. Phys. **C45**, 627 (1990).
- [18] D. Lu, A. W. Thomas, and A. G. Williams, in preparation.
- [19] A. L. Licht and A. Pagnamenta, Phys. Rev. **D2**, 1156 (1970); D. P. Stanley and D. Robson, Phys. Rev. **D26**, 223 (1982).

## TABLES

TABLE I. Helicity amplitude of delta photoproduction,  $A_{3/2}$ , in units of  $10^{-3}\text{GeV}^{-1/2}$ . Here static denotes the static calculation and PT denotes the Peierls-Thouless projection. The indices a, b, and c correspond to the Figs. 1(a), 1(b), and 1(c) respectively. The latest estimate by Particle Data Group is  $-258 \pm 6$ .

	static				PT			
R(fm)	a	b	c	total	a	b	c	total
1.0	-115	-53 -21i	-64 -18i	-205	-106	-49 -19i	-64 -18i	-195
0.9	-106	-62 -20i	-80 -20i	-216	-98	-58 -18i	-80 -20i	-205
0.8	-96	-73 -19i	-101 -21i	-233	-86	-68 -17i	-101 -21i	-222
0.7	-85	-87 -17i	-129 -22i	-260	-79	-80 -16i	-129 -22i	-249

## FIGURES

FIG. 1. Diagrams illustrating the various contributions included in the calculation. The intermediate baryons  $B$  and  $B'$  are restricted to the  $N$  and  $\Delta$  here.

FIG. 2. The recoil function  $K(r)$ , defined following Eq. (23), due to the two quark spectators in arbitrary units.

FIG. 3. The effect of the center of mass correction on the helicity amplitude,  $A_{3/2}$ , for the bare bag. The number on each curve indicates the bag radius in fm for the calculation.

FIG. 4. Individual components for the helicity amplitude,  $A_{3/2}$ , with a typical bag radius  $R = 0.8$  fm.

FIG. 5. The real parts of total  $\gamma^*N \rightarrow \Delta$  helicity amplitudes,  $\text{Re}[A_{3/2}(Q^2)]$  and  $\text{Re}[A_{1/2}(Q^2)]$ .

FIG. 6. The real part of  $\gamma^*N \rightarrow \Delta$  invariant M1 transition form factor,  $\text{Re}[G_{\Delta}^M(Q^2)]$ . Four different bag radii are used in the calculation. The experimental data are taken from Refs. [16,17].



Fig. 1

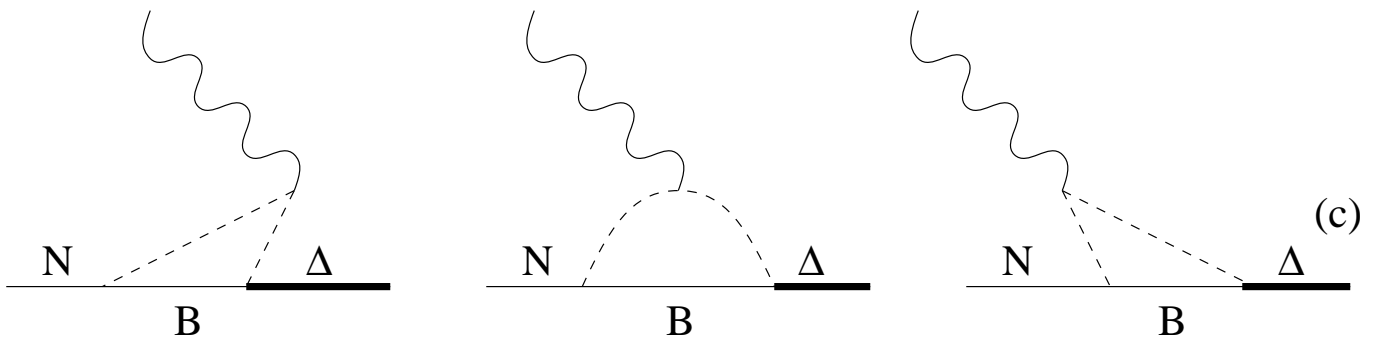
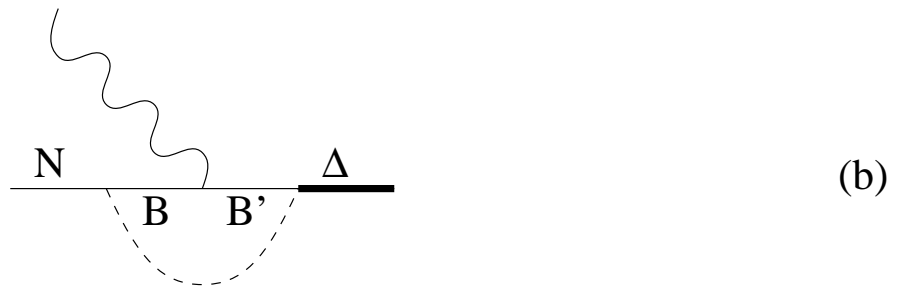


Fig. 2

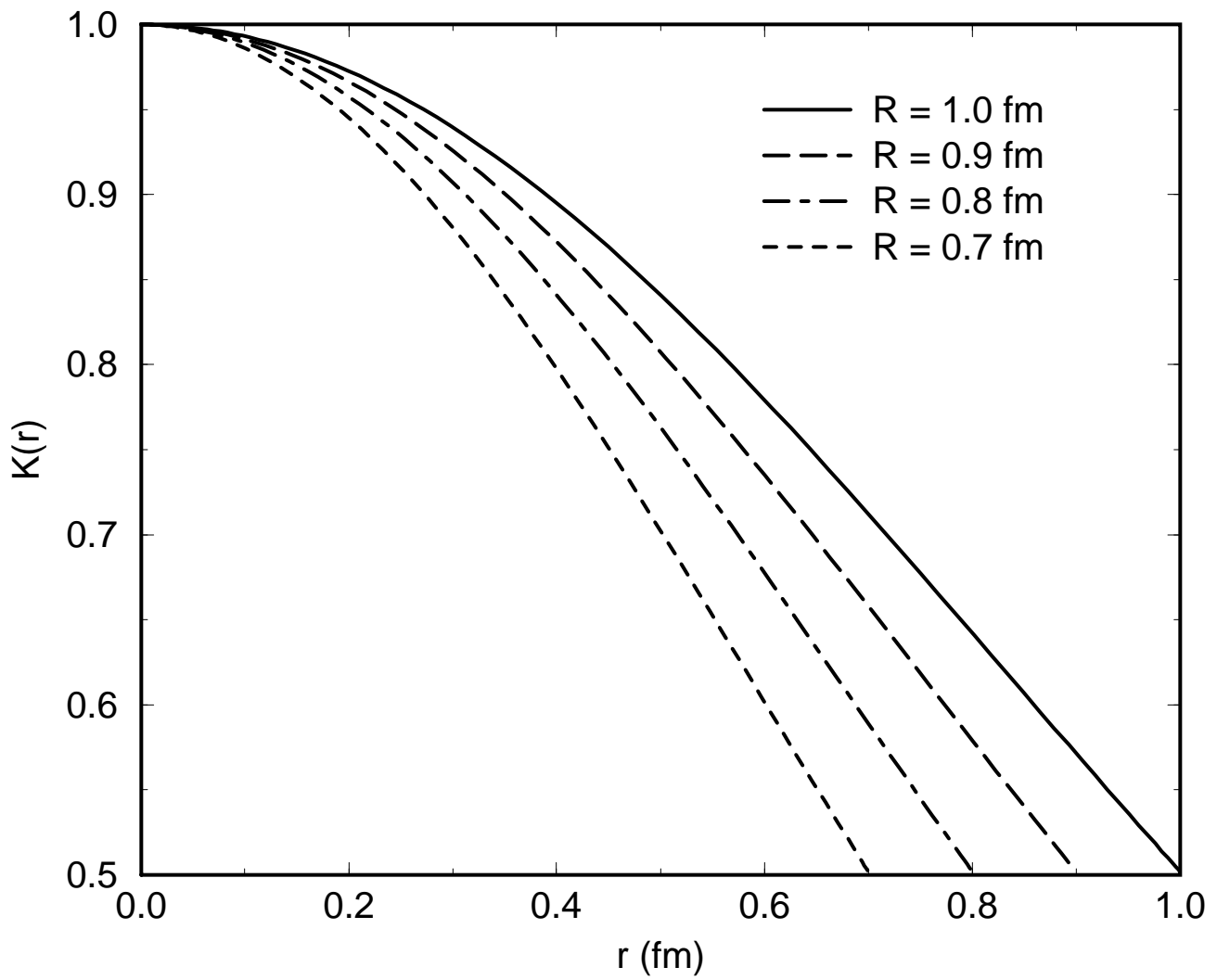


Fig. 3

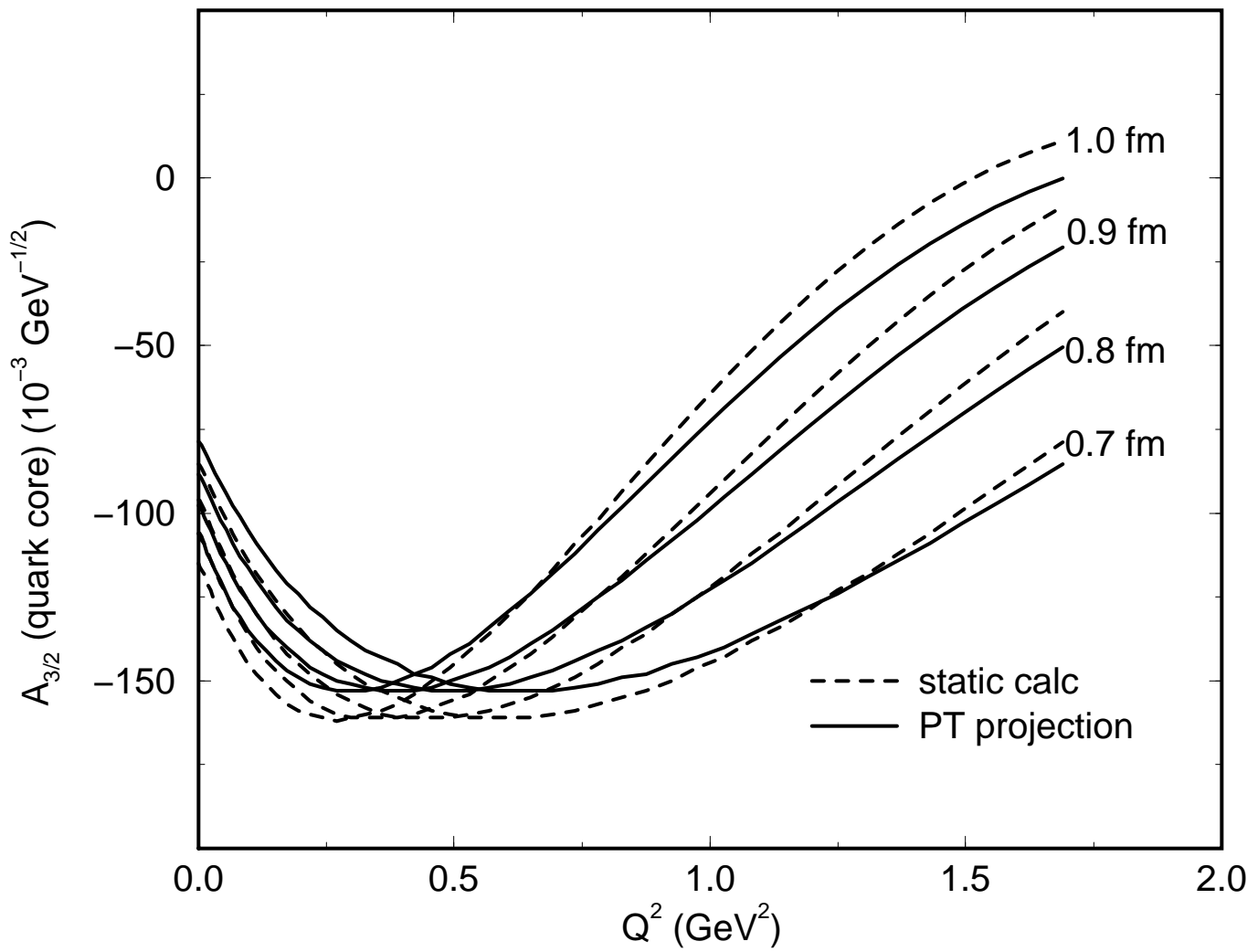


Fig. 4

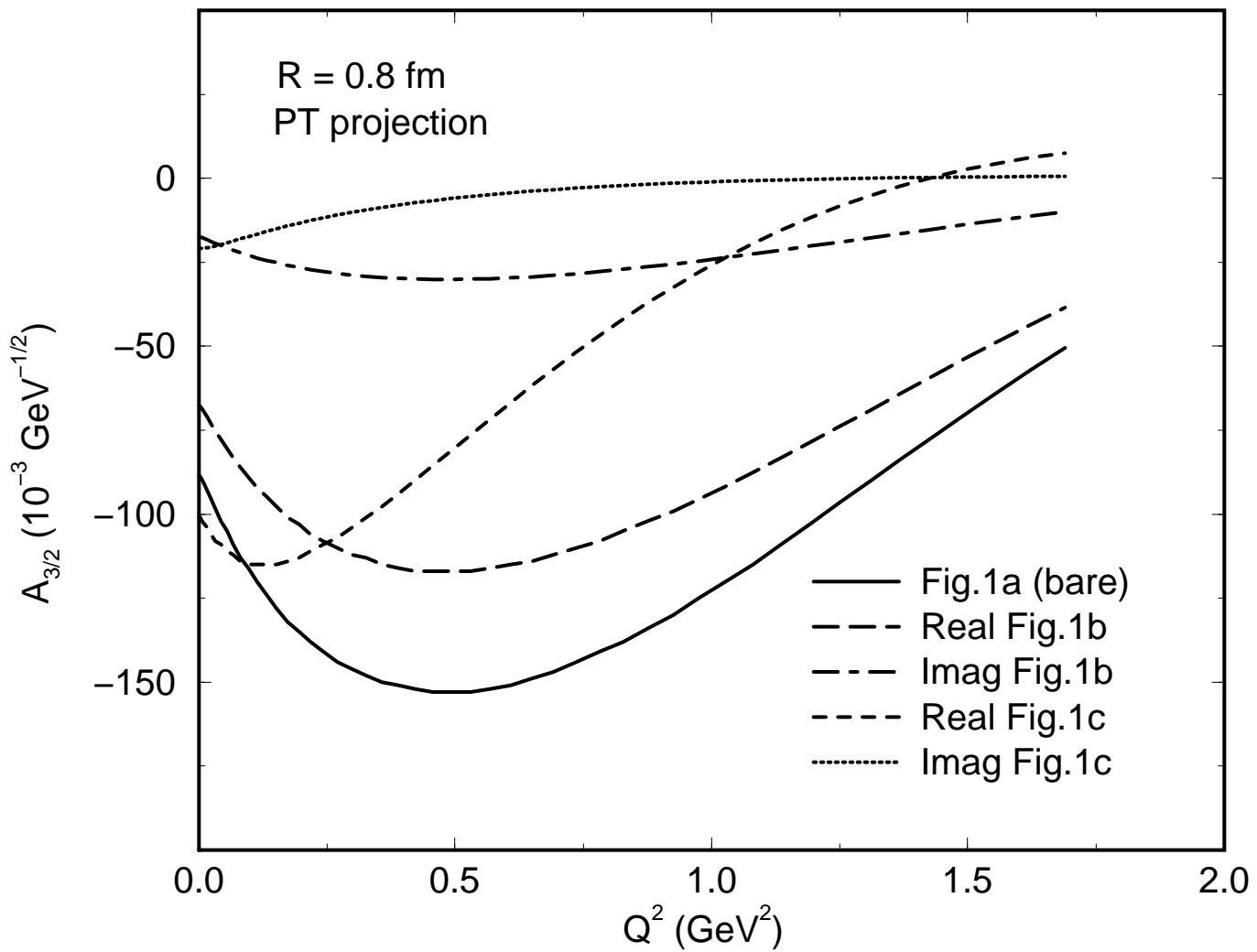


Fig. 5

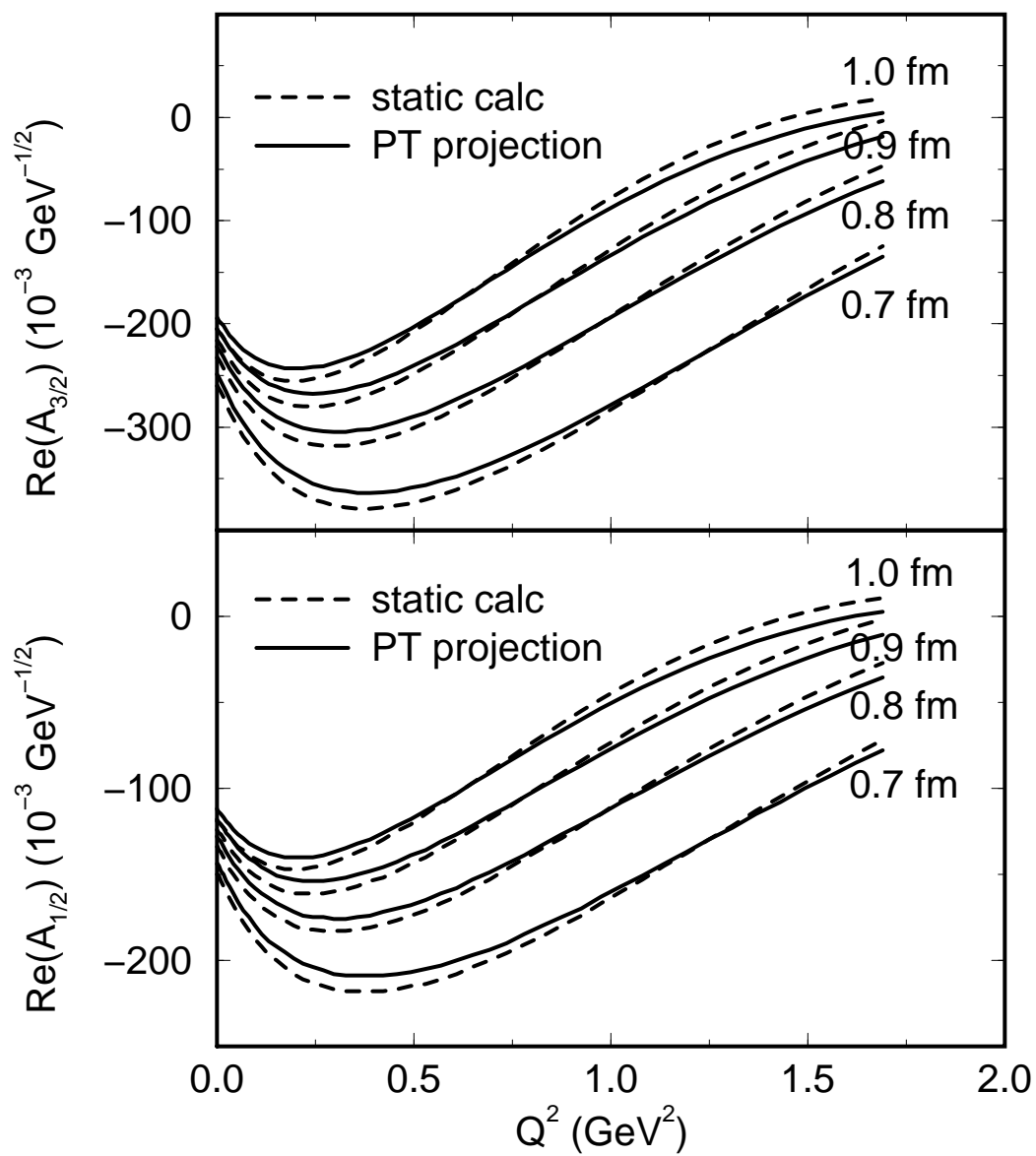


Fig. 6

